ISSN 1392–1320 MATERIALS SCIENCE (MEDŽIAGOTYRA). Vol. 17, No. 1. 2011

A Facile Method for Low-Temperature Synthesis of NaV_3O_8 as Cathode Materials for Lithium Secondary Batteries

Chao YUAN [1], Cong LI [1], Binqiang MA [1], Xin LI [1], Xiaoyu CAO [2] *

[1] *College of Sciences, Henan Agricultural University, Zhengzhou 450002, P.R. China*
[2] *School of Chemistry and Chemical Engineering, Henan University of Technology, Zhengzhou 450001, P.R. China*

Received 27 August 2010; accepted 09 October 2010

A facile method has been used to synthesize NaV_3O_8 powders with oxalic acid as the complexing agent. This soft-synthesis technique can effectively reduce the calcination temperature for synthesizing NaV_3O_8 powders to 300 °C, which is much lower than that in the solid-state synthesis. The thus-synthesized NaV_3O_8 powders are characterized by XRD, SEM and galvanostatic charge-discharge test. Among the as-prepared powders, the NaV_3O_8 powder obtained at 350 °C exhibits morphology of porous particles. The electrochemical analysis reveals that this powder demonstrates high discharge capacity and good cycleability.

Keywords: NaV_3O_8, soft-chemistry synthesis, porous particles, electrochemical performance, lithium secondary batteries.

1. INTRODUCTION

Over the past decades, sodium vanadium oxides, such as $Na_{1+x}V_3O_8$, β-$Na_xV_2O_5$ and $(Na_2O)_{0.23}V_2O_5{\cdot}xH_2O$ have been proposed as cathode materials for lithium secondary batteries due to their attractive electrochemical performances such as high discharge capacity and good cycleability [1 – 7]. Of these compounds, sodium trivanadate $Na_{1+x}V_3O_8$ with the isostructure to $Li_{1+x}V_3O_8$ is considered as a very prospective candidate as cathode material for lithium secondary batteries [1 – 5]. $Na_{1+x}V_3O_8$ as lithium intercalation host have following merits: (i) larger interlayer distance than $Li_{1+x}V_3O_8$; (ii) higher chemical diffusion coefficient of lithium than $Li_{1+x}V_3O_8$; and (iii) more reduced interaction between the interlayer cations.

However, like $Li_{1+x}V_3O_8$, the electrochemical performances of $Na_{1+x}V_3O_8$ highly depend on the adopted synthesis and processing method. In general, the $Na_{1+x}V_3O_8$ powder prepared by the high-temperature solid-state synthesis method only delivers a low capacity of about 80 $mAh{\cdot}g^{-1}$. To overcome this drawback, in this work, a wet chemistry synthesis method has been applied in the synthesis of NaV_3O_8 ($x = 0$). The structure, morphology and electrochemical properties of the as-synthesized NaV_3O_8 powders have been investigated.

2. EXPERIMENTAL

NaV_3O_8 powders were prepared by the oxalic acid-assisted liquid phase evaporation method. Fig. 1 illustrates the low-temperature preparation procedure to form target powders. First, Na_2CO_3, NH_4VO_3 and $C_2H_2O_4{\cdot}2H_2O$ were dissolved in distilled water, in the molar ratio of 1 : 6 : 4. Oxalic acid was chosen as the complexing agent. Then the three solutions were added into a beaker at 90 °C to evaporate water, leaving the homogeneous slurry. Afterwards, the obtained slurry body was dried at 110 °C to form the precursor powders. At last, the as-dried precursor powders were calcined at 250 °C ~ 350 °C for 10 h in air and then cooled to room temperature naturally to get the final NaV_3O_8 powders. The chemical reaction process for the synthesis of NaV_3O_8 can be simply expressed as

$$Na_2CO_3 + 6\ NH_4VO_3 + 4\ C_2H_2O_4 + 2\ O_2 \rightarrow$$
$$\rightarrow\ 2\ NaV_3O_8 + 6\ NH_3 + 9\ CO_2 + 7H_2O$$

For comparison, a solid-state NaV_3O_8 powder was made by heating mixed powders of Na_2CO_3 and V_2O_5 in stoichiometric amount at 620 °C for 10 h in air.

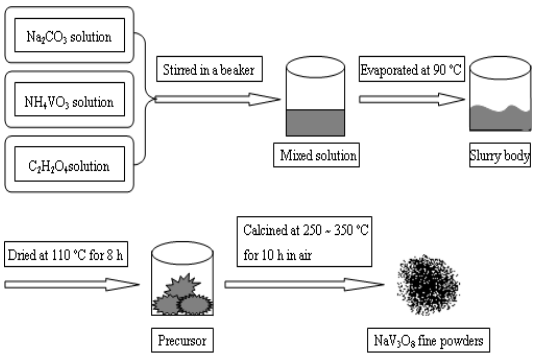

Fig. 1. Schematic representation of synthesis of NaV_3O_8 powders

The crystal structure of the synthesized powders was determined via X-ray diffraction (XRD) analysis on an XRD-Pert Pro diffractometer (XPERT PRO MPD, Netherlands) with Co Kα radiation source (λ = 1.78901 Å). To analyze the morphological feature of the synthesized powders, SEM photographs were taken by JSM6380LA (JEOL, Japan) scanning electron microscope. The electrochemical performance of the synthesized powders was evaluated by assembling CR2016 coin cells. The cathode composite composed of 80 wt% active materials, 10 wt% acetylene black and 10 wt% PTFE (microemulsion). Lithium foil was utilized as the anode, and the electrolyte solution was composed of 1 $mol{\cdot}dm^{-3}$ $LiClO_4$ dissolved in ethylene carbonate (EC) and dimethyl carbonate (DMC)

*Corresponding author. Tel.: +86-371-68756946; fax: +86-371-68756718.
E-mail address: *cxy_xll@163.com* (X. Cao)

solution (v/v, 1 : 1). The cells were galvanostatically cycled at a current density of 30 $mA \cdot g^{-1}$ within a potential range of 1.7 V to 4.0 V.

3. RESULTS AND DISCUSSION

Fig. 2 shows the XRD patterns of NaV_3O_8 powders synthesized by the oxalic acid-assisted liquid phase evaporation method at different temperatures.

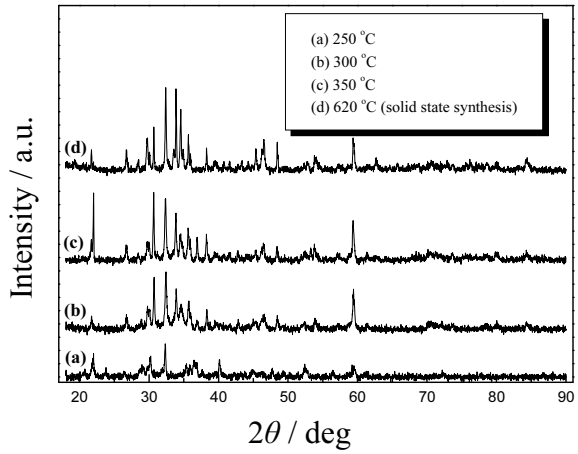

Fig. 2. XRD patterns of NaV_3O_8 powders obtained at different temperatures

It is found that some characteristic peaks of monoclinic NaV_3O_8 come to appear at the calcined temperature of 250 °C, indicating that monoclinic NaV_3O_8 begin to form at 250 °C (Fig. 2, a). With the heating temperature increasing, the relative intensities of the X-ray diffraction patterns of the NaV_3O_8 powders are becoming much stronger. In addition, it should be noted that the powder obtained at 350 °C displays the strongest diffraction line at about 2θ – 22° compared with other powders, indicating a preferred orientation of the obtained crystals. XRD result confirms that this method could result in pure NaV_3O_8 phase at lower temperature.

The morphology of NaV_3O_8 powders sintered at different temperatures is presented in Fig. 3. As seen from Fig. 3, a, the particles of the powder synthesized at 250 °C display irregular aggregation shape. It may be explained by the powder containing higher crystal water content at 250 °C. From the XRD patterns, this calcined temperature of 250 °C is not high enough to synthesize the pure phase NaV_3O_8 powders. After heating at 300 °C, particles become somewhat looser due to the dehydration. When the temperature reaches 350 °C, particles become more porous. This fact may be caused by the existence of oxalic acid. CO_2 and H_2O gas generated by metal-oxalic acid complexes can escapes from the matrix complexes when the NaV_3O_8 precursor is heated, which gives rise to the powder with porous honeycomb-like particles. In comparison with NaV_3O_8 powder prepared via the high-temperature solid-state process which completely eliminates water, the powder synthesized via this route exhibits much more disorder particle and broad size distribution.

Fig. 4 illustrates the first discharge curves of NaV_3O_8 powders synthesized at different temperatures.

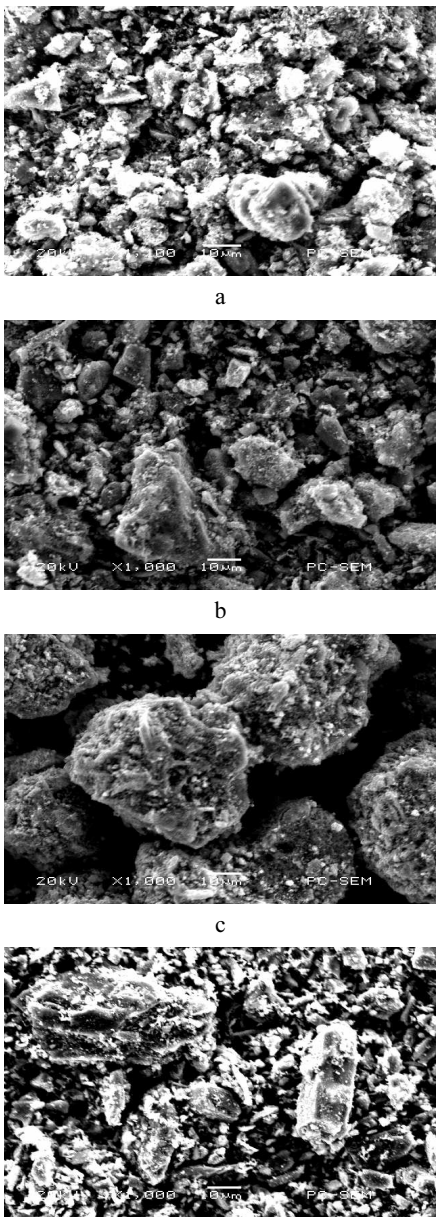

Fig. 3. SEM images of NaV_3O_8 powders obtained at different temperatures: a – 250 °C, b – 300 °C, c – 350 °C, d – 620 °C (solid state synthesis)

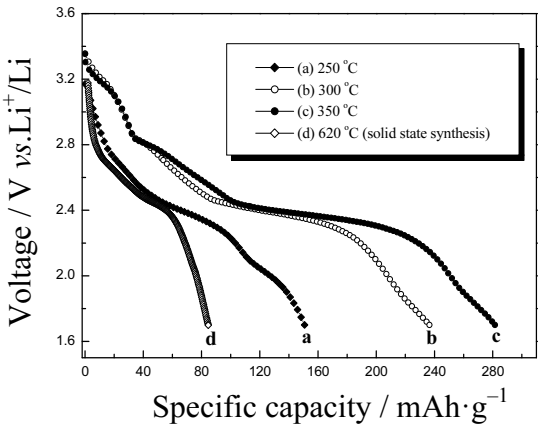

Fig. 4. The first discharge curves of NaV_3O_8 powders obtained at different temperatures

According to Fig. 4, the powders heated at 250 °C, 300 °C and 350 °C have the first discharge capacity of 150.7, 183.1 and 281.5 mAh·g^{-1}, respectively, which are much higher than that (83.6 mAh·g^{-1}) of the high-temperature solid-state synthesis powder. Among these powders, the powder obtained at 350 °C displays the highest discharge capacity and plateau. The phenomenon may be associated with the morphology features of the powder obtained at 350 °C. It is well known that the intercalation process of Li^+ ion between the cathode materials is a diffusion process, so this porous character may facilitate electrolyte soaking into particles and thus improve the diffusion kinetics of Li^+ into/out of the layered materials [8, 9]. As the high-temperature solid-state product is concerned, a reduction of some vanadium atoms from V^{5+} to V^{4+} at the temperature higher than 450 °C should be responsible for its lowest discharge capacity apart from broad particle size distribution [3].

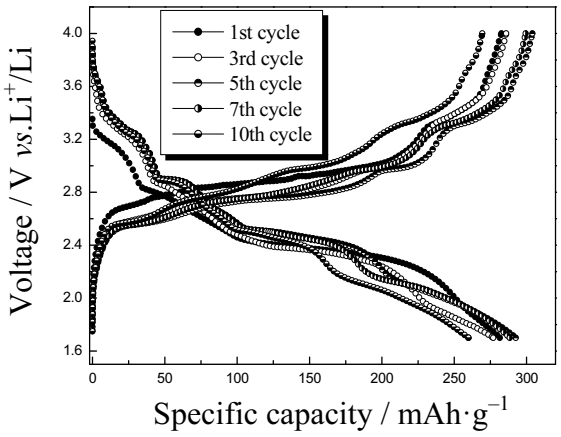

Fig. 5. Selected charge-discharge curves of NaV_3O_8 powder obtained at 350 °C

The selected discharge/charge curves of the powder synthesized at 350 °C is presented in Fig. 5. As seen in Fig. 5, the discharge/charge capacity shows a small drop and increase during the first few cycles and the fifth discharge capacity is 292.5 mAh·g^{-1}. This phenomenon is also reported by SPAHR et al. [3]. However, there is no a detailed explanation for it. Meanwhile, the electrochemical behavior of the NaV_3O_8 powder prepared at 350 °C has a certain similarity to that of $Li_{1.2}V_3O_8$ synthesized by the sol-gel route [10, 11]. Because $Li_{1+x}V_3O_8$ is isostructural to $Na_{1+x}V_3O_8$, $Li_{1+x}V_3O_8$ synthesized in wet chemical reaction system also displays the similar electrochemical behavior. We tentatively deduce that this phenomenon may be related to synthetic condition and processing method. First, H_2O, NH_3 and CO_2 inorganic molecules which are produced during the synthesis process of NaV_3O_8 may be intercalated in the puckered V_3O_8 layer, which gives rise to a pillar effect and stables the layered structure of NaV_3O_8. From the point of view of the available reversible lithium storage sites, the occupation of inorganic molecules at V_3O_8 layer is disadvantageous to Li-ion insertion at the beginning. However, these interlayer molecules are bound with NaV_3O_8 host via intermolecular interactions which are weaker than chemical bonds of inserted Li-ions and host material. Next, the inorganic molecules may be released gradually from the NaV_3O_8 host during the discharge-charge cycles. The vacated lithium insertion site leads a large amount of Li intercalation and increases discharge capacity. In addition, there are four plateaus in the voltage profiles for the lithium insertion/extraction of NaV_3O_8 powder. Moreover, it is found that the shapes of these discharge-charge curves are similar to each other, which implies that the powder synthesized at 350 °C has a good electrochemical reversibility.

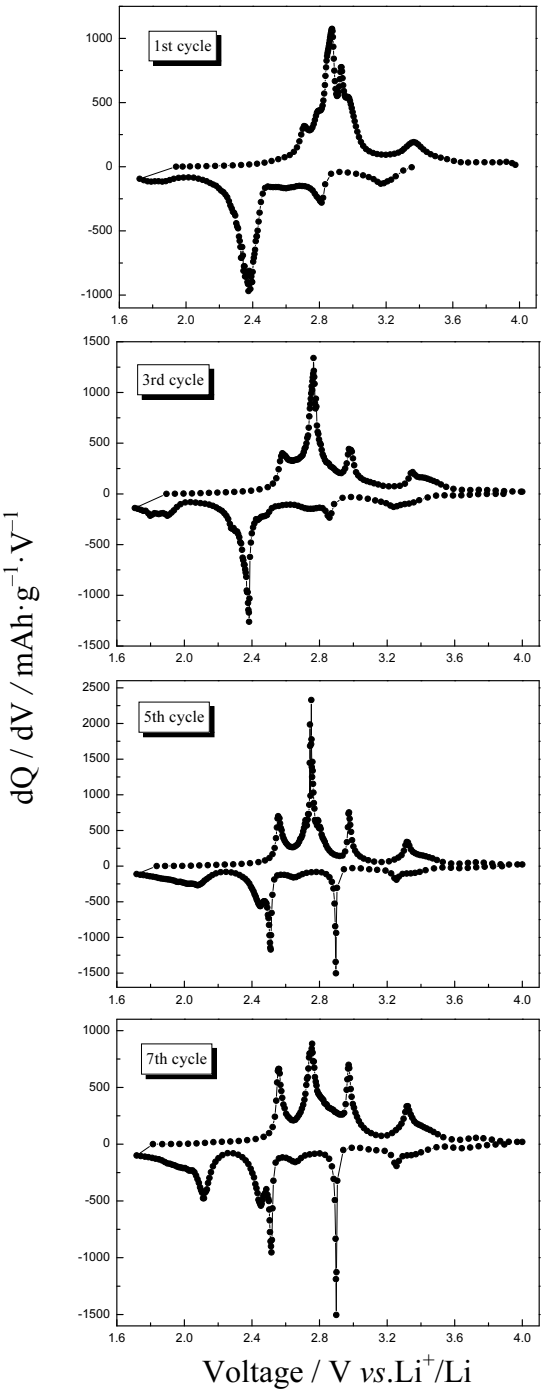

Fig. 6. Differential capacity plots s of NaV_3O_8 powder obtained at 350 °C

Fig. 6 shows the differential capacity curves of the NaV_3O_8 material obtained at 350 °C calculated from the 1st, 3rd, 5th and 7th discharge/charge curves. It is well known that the differential capacity curves indicate the reduction/oxidation potential where lithium ion is inserted

into the lattice or extracted from the lattice. As seen in Fig. 6, there are four pairs of peaks in the differential capacity plots corresponding to the plateaus in the discharge/charge curves. As the differential capacity curves of 1st cycle are concerned, there are four cathodic peaks at 3.17, 2.81, 2.37 and 1.84 V due to lithium insertion. At the same time, there are four anodic peaks at 3.37, 2.93, 2.88 and 2.71 V corresponding to the lithium extraction. However, for the 3rd, 5th and 7th cycle, the differential capacity curves display more positive reduction potentials and more negative oxidation potentials compared with the 1st cycle. For example, there are four pairs of well-defined reduction/ /oxidation peaks centered at 3.26/3.32, 2.89/2.97, 2.52/2.76 and 2.11/2.56 V for 7th cycle. The results are in good agreement with the discharge/charge study as shown in Fig. 5, indicating that NaV_3O_8 powder has the good capacity retention. The discharge capacity dependence of cycle number curves of the materials collected at a current rate of 30 $mA \cdot g^{-1}$ between 1.7 V and 4.0 V is shown in Fig. 7.

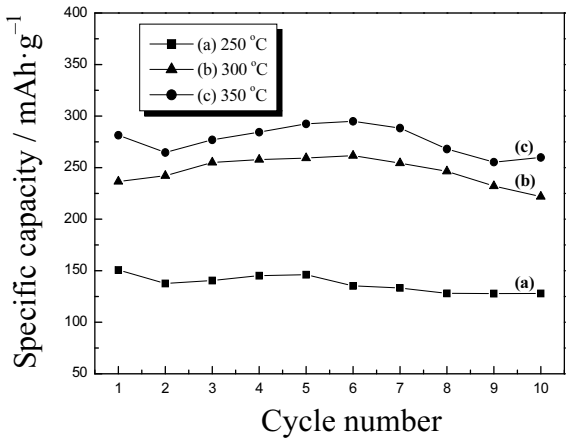

Fig. 7. Variation of discharge capacity *vs*. number of cycles using the as-synthesized powders as cathodes in the voltage range of 1.7 V to 4.0 V at a current density of 30 $mA \cdot g^{-1}$

As shown in Fig. 7, the NaV_3O_8 powders obtained at different sintered temperatures all performs a better cycling stability. The powder made at 350 °C exhibits a discharge capacity of about 259.9 $mAh \cdot g^{-1}$ within 10 cycles, demonstrating that this wet chemistry synthesis method is a promising process for obtaining porous NaV_3O_8 powders with good electrochemical performance.

4. CONCLUSIONS

In conclusion, a novel method is described for the synthesis of the layered NaV_3O_8 powders by the oxalic acid-assisted liquid phase evaporation procedure at low temperature. This wet chemistry synthesis method leads to a porous particle and high discharge capacity. It is suggested that the powder heated at 350 °C for 10 h exhibits the optimal electrochemical performances. Hence, this liquid phase evaporation method is a promising synthesis method and the NaV_3O_8 powder obtained by this method is an effective cathode material for lithium secondary batteries applications.

REFERENCES

1. **Pasquali, M., Pistoia, G.** Lithium Intercalation in $Na_{1+x}V_3O_8$ Synthesized by a Solution Technique *Electrochimica Acta* 36 (10) 1991: pp. 1549 – 1553.
2. **Pistoia, G., Li, L., Wang, G.** Direct Comparison of Cathode Materials of Interest for Secondary High-Rate Lithium Cells *Electrochimica Acta* 37 (1) 1992: pp. 63 – 68.
3. **Spahr, M. E., Novák, P., Scheifele, W., Haas, O. Nesper, R.** Electrochemistry of Chemically Lithiated NaV_3O_8: A Positive Electrode Material for Use in Rechargeable Lithium-Ion Batteries *Journal of the Electrochemical Society* 145 (2) 1998: pp. 421 – 427.
4. **Kawakita, J., Miura, T., Kishi, T.** Comparison of $Na_{1+x}V_3O_8$ with $Li_{1+x}V_3O_8$ as Lithium Insertion Host *Solid State Ionics* 124 (1 – 2) 1999: pp. 21–28.
5. **Kawakita, J., Miura, T., Kishi, T.** Effect of Crystallinity on Lithium Insertion Behaviour of $Na_{1+x}V_3O_8$ *Solid State Ionics* 124 (1 – 2) 1999: pp. 29 – 35.
6. **Apostolova, R. D., Shembel, E. M., Nagirnyi, V. M., Aurbach, D., Markovsky, B., Langzam, Y.** Synthesis and Examination of Electrolytic Sodium-Vanadium Oxide Compounds Intended for Cathodes of Lithium Batteries: The Mechanism of Formation of Electrolytic Bronze β-$Na_xV_2O_5$ *Russian Journal of Electrochemistry* 37 (10) 2001: pp. 1041 – 1049.
7. **Dai, J. X., Li, S. F. Y., Gao, Z. Q., Siow, K. S.** A New Form of Vanadium Oxide for Use as a Cathode Material in Lithium Batteries *Journal of Power Sources* 74 (1) 1998: pp. 40 – 45.
8. **Cao, X. Y., Zhan, H., Xie, J. G., Zhou, Y. H.** Synthesis of $Ag_2V_4O_{11}$ as a Cathode Material for Lithium Battery via a Rheological Phase Method *Materials Letters* 60 (4) 2006: pp. 435 – 438.
9. **Liang, H. G., Qiu, X. P., Chen, H. L., He, Z. Q., Zhu, W. T., Chen, L. Q.** Analysis of High Rate Performance of Nanoparticled Lithium Cobalt Oxides Prepared in Molten KNO_3 for Rechargeable Lithium-Ion Batteries *Electrochemistry Communications* 6 (8) 2004: pp. 789 – 794.
10. **Cao, X. Y., Xie, L. L., Zhan, H., Zhou, Y. H.** Large-Scale Synthesis of $Li_{1.2}V_3O_8$ as a Cathode Material for Lithium Secondary Battery via a Soft Chemistry Route *Materials Research Bulletin* 44 (2) 2009: pp. 472 – 477.
11. **Xie, J. G., Li, J. X., Zhan, H, Zhou, Y. H.** Low-Temperature Sol–Gel Synthesis of $Li_{1.2}V_3O_8$ from V_2O_5 Gel *Materials Letters* 57 (18) 2003: pp. 2681 – 2687.